Cairo University

Faculty of Veterinary Medicine

Department of pathology

THERAPEUTIC POTENTIALITY OF "EPIGALLOCATCHIN-3-GALLATE" AND/OR PACLITAXEL IN TARGETING CANCER STEM CELLS (CSCs) IN MAMMARY GLAND

A Thesis presented by

Heba Nashaat Ahmed Hamoudy

B.V.SC. 2009. Faculty of Veterinary Medicine Banaha University

For Master Degree in Veterinary Science
Pathology (General, Special and Post mortem)

Under Supervision of

Prof. Dr. Mohamed Mostafa Lotfy

Professor of Pathology
Faculty of Veterinary Medicine
Cairo University

Prof.Dr. Sahar Samir Mahmoud

Professor of Pathology
Faculty of Veterinary Medicine
Cairo University

Prof. Dr.Gehan Gamil Ahmed

Chief Researcher
Animal Health Research Institute,
El Dokki, Giza

(2017)

جامعة القاهرة

كلية الطب البيطرى

قسم الباثولوجيا

الامكانية العلاجية للابيجاللو كاتيكين –٣–جاليت مع/او الباكليتاكسيل في استهداف خلايا الورم الجذعية في الضرع

رسالة مقدمة من

ط.ب. هبة نشات احمد حمودي

(بكالوريوس العلوم الطبيه البيطرية جامعة بنها ٢٠٠٩)

للحصول علي
درجة الماجستير في العلوم الطبية البيطرية
تخصص باثولوجيا
(عام وخاص وتشريح مرضي)

تحت أشراف

أ.د/ محمد مصطفى لطفى
استاذ الباثولوجيا
كليه الطب البيطري- جامعه القاهرة

أ.د / سحر سمير محمود
استاذ الباثولوجيا
كليه الطب البيطري- جامعه القاهرة

أ.د/ جيهان جميل احمد
رئيس بحوث
معهد بحوث الصحة الحيوانية-الدقي

(2017)

Cairo University

Faculty of veterinary medicine

Pathology Department

Name: Heba Nashaat Ahmed Hamoudy

Date and place of birth: 16-11-1986, kaha

Nationality: Egyptian

Title of thesis:" THERAPEUTIC POTENTIALITY OF "EPIGALLOCATCHINE-3-GALLAT" and/ OR PACILTAXEL IN TARGETING CANCER STEM CELLS (CSCs) IN MAMMARY GLAND TUMORS

Scientific degree: Master's Degree (M.V.Sc.)

Supervisiors:

Prof. Mohamed Mostafa Lotfy

Professor of Pathology, Faculty of Veterinary Medicine, Cairo University

Prof. Dr. Sahar Samir Mahmoud

Professor of Pathology, Faculty of Veterinary Medicine, Cairo University

Prof. Dr. Gehan Gamil Ahmed

Chief Researcher, Pathology department, Animal Health Research Institute, Dokki, Giza

Abstract

Cancer stem cells (CSCs) are a subpopulation of tumor cells that own self-renewal capability, tumor recurrence and metastasis as well as resistance to current cancer therapies. Epigallocatechin-3-gallate (EGCG) is a type of catechin found in green tea that is known by its powerful chemoprotective ability. Hence, the current study aimed to focus on the effect of EGCG on 7,12 Dimethyl-benzanthracene (DMBA) -induced tumor metastasis, angiogenesis and CSCs. For these reasons both *in vitro* and *in vivo* studies were carried out. The *in vitro* evaluation of the effect of the used chemicals (paclitaxel, EGCG and their combination) at different doses on one of the breast cancer cell line, MCF-7 was carried out to evaluate the cell viability and apoptosis. The highest significant alterations in cellular morphology were observed on the sole use of EGCG followed by combined use of both paclitaxel and EGCG, while the use of paclitaxel alone showed the least effect. It was observed that the later cellular alterations were dose related. *In vivo* studies, therapy was started in 3 groups of DMBA-induced mammary cancer in virgin female rats using EGCG, paclitaxel or their combination. It was found that EGCG exhibited significant chemopreventive

effects and anti-CSCs activity through several pathways including significant decrease in the size and number of tumors/ rat, significant amelioration of the oxidative stress markers' alterations as well as significant inhibition of CD44, VEGF, Ki-67 and MMP-2 expression associated with significant increased expression of caspase-3. In addition, the combination of EGCG to paclitaxel significantly enhanced the later anticancer efficacy. Herein it is concluded that EGCG could be offered as an unprecedented curative strategy to eradicate cancer.

Keywords: Cancer stem cells (CSCs), EGCG, antioxidant, Ki-67, CD44, mammary tumor.

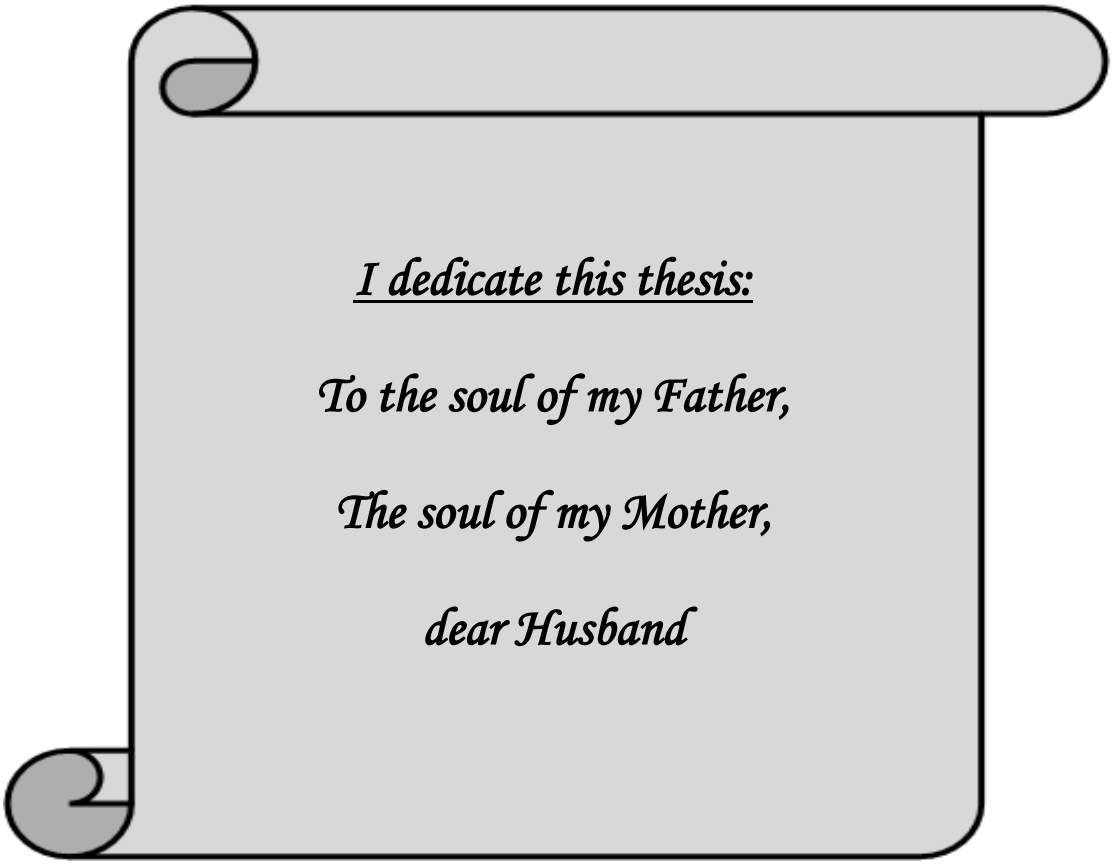
I dedicate this thesis:
To the soul of my Father,
The soul of my Mother,
dear Husband

Acknowledgement

First of all, my deep prayerful gratitude should be submitted to merciful GOD whose help I always seek and without his willing I will achieve nothing.

My deepest gratitude and faithful thank to ***Prof. Dr. Prof. Mohamed Mostafa Lotfy*** *professor of pathology, faculty of veterinary medicine, Cairo University for his supervision, continuous aid and fruitful advice, great help and encouragement during course of this work.*

My deepest gratitude and faithful thank to ***Prof. Prof. Dr. saher Samir mahmoud,*** *professor of pathology, faculty of veterinary medicine, Cairo University for his supervision, continuous aid and fruitful advice, great help and encouragement during course of this work.*

I would like to express my deep appreciation and gratitude to ***Prof. Dr. Gehan Gamil Ahmed****, professor of pathology, Animal Health Research Institute, Dokki, Giza and Great gratitude for all staff members of pathology, Animal Health Research Institute, Dokki, Giza.*

I would like to acknowledge the ***Research Park, Faculty of Agriculture, Research lab, Cairo university*** *for its great role in culture and assessment of cancer cell line and culture; and its great help in management of the in vitro study.*

List of Content

Introduction…..……..…..……...……1
Review of literature .....……..…….……3
A. Stem cells in normal mammary gland and breast cancer……...3

B. (1). Cancer stem cells (CSCs)……..……..….3
B. (2). Models for Tumor Propagation.....5
B. (3). Heterogeneity or identification of CSCs (CSC markers).....5
B. (4). Biological Significance of cancer stem cells plasticity.....7
B.(5). Pathological significance of mammary cancer stem cells……10
B. (6). Isolation and In vitro propagation of tumorigenic Breast Cancer Cells with Stem/Progenitor Cell properties...…….....10

C. Mammary gland tumors in animals..……11

C. (1). Defention of mammary tumors.……..……11
C. (2). Incidence of mammary tumors...…….....11
C. (3). Classifications of mammary gland tumors….……....12
a. BENIGN TUMORS…….…….....12
a. (1). Simple adenoma…..……..…..…13
a. (2). Ductal Adenoma…….....13
a. (3). Intraduct papillary adenoma…..……...…...13
a. (4). Fibroadenoma……..……..….13

b. Malignant mammary tumors, Classification, Types and Metastasis……..……..…..14
b. (1). Adenocarcinoma... ..……..……15
b. (2). Papillary adenocarcinoma……15
b. (3). Complex papillary adenocarcinomas…….……...15
b. (4). Solid carcinoma…….…….....16
b. (5). Comedo-carcinoma …….……...….....16
b. (6). Carcinoma–Cribriform…..…….....16
b. (7). Anaplastic carcinoma..……..…..16
D. Etiology of mammary gland tumors……..17
D. (1). Hormonal factors...……..……17
D. (2). Physical carcinogen...……..…….....17
D.(3). Gene mutations as commencement of carcinogenesis……..…..18
D. (4). Tumor viruses…….....18
D. (5). Immunological factors……..……...19
D. (6). Chemical carcinogens...……..……...….19

E. Induction of experimental mammary carcinogenesis in rats with 7, 12-dimethylbenz (a) anthracene (DMBA)…….20

F. Current recommendations for mammary gland tumors……..21
F. (1). Surgery ……..……..**.....**21
F. (2). Adjuvant therapies**...**……..……22
F.(3). Phytochemicals as a novel treatment for breast cancer……..…….…23

G. Mechanisms of green tea components action on breast cancer……25
G. (1). Anti-angiogenesis**..**……..…...25
G. (2). Interactions with target proteins……..……...26
G. (3). Inductions of cell cycle arrest and apoptosis……26
G.(4). Tea Polyphenols and Inhibition of Oncogene expression…….…27
G. (5). targeting multi drug resistance…..……..**..**27
G. (6). anti-oxidant properties of polyphenols……..…27

Materials and methods……...…..…….…….**.....**29

Results…..…..……..…….**.....**38
I. Results of in-vitro studies by using (MCF-7) cell line……**..**38
I. 1. The cytotoxic effect of the tested chemicals (paclitaxel and / or EGCG) on MCF-7 cell line at different doses**...**……..38
I. 2. Results of the viability test of MCF7 cell line treated with the different doses of the tested chemicals (paclitaxel and / or EGCG) using neutral red uptake assay…….....**.....**43
I. 3. Results of IC50 (the half maximal inhibitory concentration) of the tested chemicals (paclitaxel and / or EGCG) on MCF7……..……**.**45
II. Results of In-vivo study……**...**46
II. 1.Results of clinical examination and mortalities in DMBA control group as well as the different treated groups……..…46
II. 2.Results of tumor volume and follow up in DMBA control group as well as the different treated groups..…….……..….**.**46
II. 3. Results of antioxidant markers…….……48
II. 4. Pathological findings……50
Discussion……94
Conclusion...……..……102
Summary …..……**....**103
References...……..……105
الملخص العربي……..2
المستخلص العربي…..……1

List of Figures

Fig.1: Negative control: MCF-7 cell line normal showing sheet of spindle cells and no alterations in the morphology (100 x magnifications).	39
Fig.2: MCF7 cell line treated with (20µM EGCG) showing moderate alteration in the cellular morphology such as cellular rounding and vacuolation (200 x magnifications).	39
Fig.3: MCF7 cell line treated with (40µM EGCG) showing severe growth inhibition, rounding and detachment (100 x magnifications).	40
Fig.4: MCF7 cell line treated with (0.5µM paclitaxel +20µM EGCG) showing cellular rounding cells and detachment (200 x magnifications).	40
Fig.5: MCF7 cell line treated with a mixed dose of (1 µM paclitaxel+ 20 µM EGCG) showing severe cellular alterations and detachment (100 x magnifications).	41
Fig.6: MCF7 cell line treated with (0.5µM paclitaxel) showing mild alterations in cellular morphology and apoptosis (200 x magnifications).	41
Fig.7: MCF7 cell line treated with (1µM paclitaxel) showing marked cellular vacuolation (200 x magnifications).	42
Fig.8: MCF7 cell line treated with (2µM paclitaxel) showing cellular vacuolation and clumbing (200 x magnifications).	42
Fig.9: Showing severe decrease in the viability of MCF7 cell line with increased the dose of EGCG compared to control.	44
Fig.10: Showing that the viability of MCF-7 cell line was poorly affected by the sole paclitaxel treatment.	44
Fig.11: Showing that the IC50 of the different doses of paclitaxel which was 2.3µM	45
Fig.12: Showing that the IC50 of different doses of EGCG which was 24.5 µM.	45
Fig.13: Showing the tumor volume (mm^3) in DMBA control group and the different treated groups along the therapy period	47
Fig.14: Plasma MDA nmole/g level and GSH nmole/g content in the negative control, DMBA control and different treated groups.	49
Fig.15: Plasma catalase activity (u/g) in the negative control, DMBA control and different treated groups.	49
Fig. 16: Mammary gland of the control negative rat showing normal alveoli and milk ducteols with normal stroma (H&E, X 100).	50
Fig.17: Mammary gland of the DMBA control rat at the end of the experimental period showing large tumor in the anterior lobes of the mammary gland which were lobulated and eventuated in the skin.	51
Fig. 18: Mammary gland of DMBA control group showing, ductal epithelial reaction; moderate hyperplasia with some cellular atypia and cellular debris in the lumen (H&E, X 200).	53

Fig. 19: Higher magnification of fig.18 showing, cellular atypia and other epithelial reaction (H&E, X 400).	53
Fig. 20: The neoplastic cells appeared basophilic with vacuolated or foamy appearance of the cytoplasm and pleomorphic nuclei mostly round, oval, vesicular and hyperchromatic with prominent nucleoli (H&E, X 400).	54
Fig. 21: Solid type adenocarcinoma in mammary gland of DMBA control rat showing; rounded masses of tumor cells with little glandular formation, most of cells were large pleomorphic with pleomorphic, hyper chromatic or vesicular nuclei (H&E, X 400).	54
Fig. 22: Solid type adenocarcinoma in mammary gland of DMBA control rat showing; solid rounded masses of anaplastic tumor cells, notice the great cellular pleomorphic (H&E, X 400).	55
Fig. 23: Solid type adenocarcinoma in mammary gland of DMBA control rat showing; solid rounded masses of tumor cells separated by thin fibrous bands. Tumor cells were prominent increased mitotic activity, pleomorphism, increased in the sizes and number of nuclei of the tumor cell and metachromatic material (H&E, X 400).	55
Fig.24: Cribriform type adenocarcinoma in mammary gland of DMBA control rat showing; numerous variable sizes small rounded spaces in the tumor mass (H&E, X 200).	56
Fig.25: Cribriform type adenocarcinoma in mammary gland of DMBA control rat showing; numerous variable sizes small rounded spaces in the tumor mass. Cell different in shapes, sizes and hyperchromatic nuclei, increased mitotic division (H&E, X 400).	56
Fig.26: Cribriform type adenocarcinoma in mammary gland of DMBA control rat showing; numerous variable sizes small rounded spaces in the tumor mass. Tumor masses appeared sieves like (H&E, X 400).	57
Fig.27: Comedo-form type adenocarcinoma in mammary gland of DMBA control rat showing; centrally located comedo-necrosis in the sheet of the neoplastic cells (H&E, X 200).	57
Fig.28: Comedo-form type adenocarcinoma in mammary gland of DMBA control rat showing; the located comedo-necrosis appeared as areas of eosinophilic cellular debris centrally located in the tumor masses (H&E, X 200).	58
Fig.29: Higher magnification of fig.29 showing; centrally located comedo-necrosis appearing as area of eosinophilic cellular debris. Noticed the characters of nuclear malignancy (H&E, X 400).	58
Fig.30: Comedo-form type adenocarcinoma in mammary gland of DMBA control rat showing; squamous metaplasia in the comedo form pattern (H&E, X 400).	59
Fig.31: Mammary gland of DMBA control group showing; both cribriform adenocarcinoma and comedo-form adenocarcinoma (H&E, X 400).	59
Fig.32: Mammary gland of DMBA control rats showing; cystic carcinoma, the	60

tumor cells were separated by cystic spaces that filled with eosinophilic material (H&E, X 400).	
Fig.33: Mammary gland of DMBA control group showing; heavy stromal reaction of marked mononuclear cells infiltrated around the neoplastic mass with free RBCs (H&E, X 400).	60
Fig.34: Mammary gland of DMBA control group showing; heavy stromal reaction of marked mononuclear inflammatory cells infiltrated around the neoplastic mass (H&E, X 400).	61
Fig. 35: Lung of DMBA control rat showing; metastatic foci of tumor cells in the lung tissue with variable degrees of congestion, hemorrhage and pulmonary edema. (H&E, X 400).	61
Fig.36: Lung of DMBA control rat showing; tumor emboli of neoplastic cells inside lymph vessels in a case of lung metastasis (H&E, X 200).	62
Fig.37: Lung of DMBA control rat showing; tumor emboli of neoplastic cells inside lymph vessels in a case of lung metastasis (H&E, X 400).	62
Fig. 38: Lung of DMBA control rat showing; metastatic foci of tumor cells in the lung tissue with variable degree of congestion and pulmonary edema. (H&E, X 400).	63
Fig. 39: Mammary gland of EGCG treated rat before starting therapy (A) and four weeks post therapy (B) notice marked reduction in tumor size.	64
Fig. 40: Mammary gland of EGCG treated rat showing replacement of tumor masses by proliferated more collagenous connective tissue and spares tubular structures lined by necrotic cells (H&E, X100).	65
Fig. 41: Mammary gland of EGCG treated rat showing; markedly necrosis, vacuolation and desquamation of the neoplastic cells in the sequestered alveolar structures (H&E, X200).	65
Fig. 42: Mammary gland of EGCG treated rat showing; markedly nuclear pyknosis, vacuolation and desquamation of the neoplastic cells in the sequestered alveolar structures (H&E, X 400).	66
Fig. 43: Mammary gland of EGCG treated rat showing; markedly fibrous proliferation among the groups of necrotic neoplastic cells (H&E, X 200). .	66
Fig. 44: Mammary gland of EGCG treated rat showing; the blushed coloured proliferated more collagenous fibrous tissue replacing the tumor mass (Masson's trichrome stain, X200).	67
Fig. 45: Mammary gland of EGCG treated rat showing; replacement of the tumor mass with blushed coloured proliferated more collagenous fibrous tissue with sparse of tubular structures lined by necrotic cells. Bluish coloured proliferated fibrous bands replacing the neoplastic cell (Masson's Trichrome stain, X 200).	67
Fig. 46: Mammary gland of EGCG treated rats showing; great replacement of the tumor mass with proliferated fibrous tissue, notice the remaining neoplastic cells appeared as nests of sequested tubules (Masson's Trichrome	68

stain, X 400).	
Fig. 47: Mammary gland of paclitaxel treated rat before starting therapy (A) and four weeks post therapy (B) showing the slightly decrease In the tumor growth.	69
Fig. 48: Mammary gland of paclitaxel treated rat showing; variable degree of necrosis and desquamation of the neoplastic cells (H&E, X200).	70
Fig. 49: Mammary gland of paclitaxel treated rat showing; necrosis of the neoplastic cells with fine bands of fibrous connective tissue encircling the necrosed tumor cells. (H&E, X400).	70
Fig. 50: Mammary gland of paclitaxel treated rat showing; large area of cellular necrosis of the neoplastic cells surrounded by proliferated fibrous connective tissue (H&E, X400).	71
Fig. 51: Mammary gland of paclitaxel treated rat showing; vacuolation nuclearpyknosise and desquamation of the neoplastic cells with high apoptotic bodies and necrotic debris. (H&E, X400).	71
Fig. 52: Liver of paclitaxel treated rat showing; dilatation of hepatic sinusoids, congestion of central vein and disorganization of hepatic cords. (H&E, X 200).	72
Fig. 53: Liver of paclitaxel treated rat showing; severe congestion of central vein and hepatic sinusoids, marked vacuolar degeneration of hepatocytes as well as many necrotic cells (H&E, X 400).	72
Fig. 54: Lung of paclitaxel treated rat showing; severe congestion, pulmonary edema and proliferation of interstitial tissue (H&E, X 200).	73
Fig. 55: Kidney of paclitaxel treated rat showing; wide spread hyalinization of renal tubular epithelium, vacuolated cells and intertubular edema (H&E, X 400)	73
Fig. 56: Kidney of paclitaxel treated rat showing; marked necrosis and hyalinization the tubular epithelium, mesangeal necrosis and beginning of esinophilic cast formation in the Bowman's space (H&E, X400).	74
Fig. 57: Mammary gland of combined therapy rat before starting therapy (A) and four weeks post therapy (B) notice the marked reduction the tumor size.	75
Fig. 58: Mammary gland of the combined (EGCG and paclitaxel) treated rat showing extensive nuclear pyknosis and granular eosinophilic areas of necrosis as well as peripheral congestion (H&E, X100).	76
Fig. 59: Mammary gland of the combined (EGCG and paclitaxel) treated rat showing extensive necrosis of the neoplastic cells and appearance of granular eosinophilic area of necrosis (H&E, X200).	76
Fig. 60: Higher magnification of Mammary gland of combined (EGCG and paclitaxel) treated rat showing; necrosis and desquamation of neoplastic cells (H&E, X400).	77
Fig. 61: Mammary gland of the combined (EGCG and paclitaxel) treated rat showing marked vacuolation as ghost, haphazard arrangement and extensive nuclear pyknosis, granular eosinophilic areas of necrosis (H&E, X400)**.**	77

Fig. 62: Liver of combined (EGCG and paclitaxel) treated rat showing; moderate degree of hepatocellular vacuolar degeneration and necrosis with dilatation of hepatic sinusoid (H&E, X200).	78
Fig. 63: Kidney of combined (EGCG and paclitaxel) treated rat showing; moderate necrobiotic changes of renal epithelium linings, intertubular pockets of hemorrhages and granular renal cast in the lumen of some tubules (H&E, X400).	78
Figure 64: Section of mammary tumor of DMBA control rat showing marked CD44 positive cells at the periphery of the tumor mass. **(X 400).**	80
Figure 65: Section of mammary tumor of DMBA control rat showing marked CD44 positive cells in the stromal tissue at the periphery of the tumor. **(X 400).**	80
Figure 66: Section of mammary tumor of DMBA control rat showing scattered CD44 positive cells in the entire of the tumor mass. **(X 400).**	81
Figure 67: Section of supra mammary lymph node of DMBA control rat showing marked expression of CD44 in the sinuses and at the periphery. **(X 400).**	81
Figure 68: Section of supra mammary lymph node of DMBA control rat showing marked expression of CD44. **(X 600).**	82
Figure 69: Section of mammary tumor of EGCG treated rat showing negative expression of CD44 among the degenerated and necrotic neoplastic cells. **(X 200).**	82
Figure 70: Section of mammary tumor of paclitaxel treated rat showing positive expression of CD44 in the cytoplasm of large cells. **(X 600).**	83
Figure 71: Section of mammary tumor of both EGCG and paclitaxel treated rat showing rare positivity of CD44. **(X 400).**	83
Figure 72: Section of mammary tumor of DMBA control rat showing marked positive expression of VEGF in the endothelial linings the blood vessels in the vicinity of the tumor mass. **(X 400).**	84
Figure 73: Section of supra mammary lymph node of DMBA control rat showing marked peripheral positivity of VEGF especially in the subcapsular sinuses. **(X 600).**	84
Figure 74: Section of supra mammary lymph node of DMBA control rat showing peripheral positivity of VEGF. **(X 400).**	85
Figure 75: Section of mammary tumor of paclitaxel treated rat showing positive VEGF expression in the endothelial linings the blood vessel. **(X 400).**	85
Figure 76: Section of mammary tumor of DMBA control rat showing positive expression of MMP-2 in the tumor mass. **(X 600).**	86
Figure 77: Section of mammary tumor of DMBA control rat marked immune positivity of MMP-2 in the neoplastic cells. **(X 600).**	86
Figure 78: Section of tumor of paclitaxel treated rat showing scattered expression of MMP-2 among the degenerated and neoplastic cells. **(X 400)**	87
Figure 79: Section of mammary tumor of DMBA control rat showing wide	87

spread immunopositivity of Ki-67 among the neoplastic cells. **(X 200).**	
Figure 80: Section of supra mammary lymph node of DMBA control rat showing marked diffuse immunopositivity of Ki-67. **(X 400).**	88
Figure 81: Section of mammary tumor of EGCG treated rat showing obvious nil expression of Ki-67. **(X 400).**	88
Figure 82: Section of mammary tumor of DMBA control rat showing immune-negative caspase-3 expression. **(X 400).**	89
Figure 83: Section of mammary tumor of EGCG treated rat showing immunopositivity of caspase-3. **(X 600).**	89
Figure 84: Section of mammary tumor of EGCG treated rat showing wide spread immunopositivity of caspase-3. **(X 400)**	90
Figure 85: Section of mammary tumor of paclitaxel treated rat showing moderate immunepositivity of caspase-3. **(X 200).**	90
Figure 86: Section of mammary tumor of both EGCG and paclitaxel treated rat showing marked expression of caspase-3. **(X 600).**	91
Fig. 87: Showing proliferation and apoptotic index in the DMBA control group and other various treated groups.	93

List of abbreviations

EGCG	Epigallocatechin gallate green tea
CSCs	Cancer stem cells
MRP1	Multi-drug resistance associated protein 1
P-gp	P-glycoprotein
BCRP	Breast Cancer Resistance Protein
VEGF	Vascular endothelial growth factor
TDLU	Terminal duct lobular unit
CLL-1	C-type lectin-like molecule-1
EMT	Epithelial mesenchymal transition
ABC	ATP-Binding –Cassette transporters
MET	Mesenchymal epithelial transition
HIFs	hypoxia-inducible factors
NF-κB	Nuclear factor kappa B
cIAPs	cellular inhibitors of apoptosis
DMBA	7, 12-dimethylbenz (a) anthracene
EC	Epicatechin
HIF-1α	Hypoxia inducible factor alpha
GRP78	glucose-regulated protein 78
JNK	Jun N-terminal kinases
MMP-9	Matrix metalloproteinase
MXR	Mitoxantrone resistance protein
MDR	Multi Drug resistance
ROS	Reactive oxygen species
DMEM	Dulbeco's modified eagle media
EDTA	Ethylenediamine tetra acetic acid
MDA	Malondialdehyde level
CAT	catalase activity
GSH	Glutathione content
TDs	Terminal ducts
Abs	Alveolar buds
HA	Hyaluronic acid
MCF-7	Michigan Cancer Foundation-7
TNM	Tumor Lymphnodes Metastasis